Geoderma 363 (2020) 114168

Contents lists available at ScienceDirect

Geoderma

journal homepage: www.elsevier.com/locate/geoderma

Using depression deposits to reconstruct human impact on sediment yields from a small karst catchment over the past 600 years

Yunqi Zhang[a], Yi Long[b,*], Xinbao Zhang[b], Zengli Pei[a], Xue Lu[a], Zhehong Wu[a], Mingyang Xu[a], Haiquan Yang[c], Peng Cheng[d]

[a] College of Forestry, Sichuan Agriculture University, Chengdu 611130, China
[b] Institute of Mountain Hazards and Environment, Chinese Academy of Sciences, Chengdu 610041, China
[c] State Key Laboratory of Environmental Geochemistry, Institute of Geochemistry, Chinese Academy of Sciences, Guiyang 550081, China
[d] State Key Laboratory of Loess and Quaternary Geology, Institute of Earth Environment, Chinese Academy of Sciences, Xi'an 710000, China

ARTICLE INFO

Handling Editor: Morgan Cristine

Keywords:
Karst depression
Sedimentation rate
Specific sediment yield
Huguang to Sichuan migration
Charcoal fragment

ABSTRACT

Assessment of long-term human impact on sediment yields from karst settings can improve our understanding of the pattern of soil erosion causing rocky desertification in the historical context of environmental change influenced by human activity. Few previous investigations have estimated this impact over time-scales longer than 50 years. This study used dated depression deposits to reconstruct human impact on sediment yields from a small karst catchment in the Three Gorges Reservoir Region, China, over the past 600 years. ^{137}Cs, $^{210}Pb_{ex}$, and ^{14}C techniques were used to determine short-term (~50 yr), medium-term (~100 yr), and long-term (~600 yr) sedimentation in the karst depression, respectively. Sedimentation rates and specific sediment yields in the catchment during six distinct stages (1351–1462, 1463–1701, 1702–1809, 1810–1916, 1917–1962, and 1963–2017) were determined from core samples. The results indicate that soil loss during the period 1351–1962 was more intensive than that since 1963, which reveals changing sediment yields impacted by human activity over the past 600 years. The high values during the three stages before 1810 can be attributed to the impacts of large-scale migration of people from Huguang to Sichuan during the Ming and Qing dynasties; the higher values during 1810–1916 might reflect increasing disturbance related to rapid population expansion; the highest values (1917–1962) were caused by large-scale deforestation in 1958 and a consistently increasing population; and low values since 1963 reflect constraints on the supply of sediment source materials. These results suggest that rocky desertification might be a long-term land-surface process induced by human activity over timescales of > 100 years rather than a short-term modern process occurring over a number of decades. This is the first attempt to examine the long-term history of human impact on sediment yields from a karst catchment using depression deposits. This work improves our understanding of the influence of human activities on soil loss at a depression-catchment scale, and of the evolution and dynamics of rocky desertification in karst areas.

1. Introduction

Karst landscapes cover ~12% of the total land area worldwide and ~36% of the area in China (Yuan, 2006; Dai et al., 2017). Karst environments are generally characterized by low rates of soil formation, thin soil layers, exposed and subsurface structures, rugged and complex terrain, and fragmented landscapes comprising patchy croplands and scattered rock outcrops (Wang et al., 2004; Ford and Williams, 2013; Yang et al., 2016; Li et al., 2017). Constant erosion in karst environments can eventually result in rocky desertification, that is, the transformation of a karst area covered by vegetation and soil into a rocky landscape almost devoid of soil and vegetation. Such desertification has occurred in many karst areas in China mainly as a result of intensive farming (Jiang et al., 2014; Li et al., 2018, 2019a). The impact of human activity on sediment yields and the threat of the rocky desertification of karst areas that support human wellbeing are of increasing concern.

It is generally difficult to obtain reliable sediment yield data from karst regions because of the fragmented landscape and double-spaced structures above and below ground-level (Wang et al., 2004; Bai et al., 2010, 2013; Ford and Williams, 2013). Depressions are a landform unit characteristic of karst regions, with hill-slope soil losses often forming deposits within these depressions. These depression deposits document the history of sediment yield from the contributing catchment(s).

* Corresponding author at: Institute of Mountain Hazards and Environment, Chinese Academy of Sciences, No. 9, Block 4, Renminnanlu Road, Chengdu, China.
E-mail address: longyi@imde.ac.cn (Y. Long).

https://doi.org/10.1016/j.geoderma.2019.114168
Received 1 August 2019; Received in revised form 6 November 2019; Accepted 29 December 2019
Available online 16 January 2020
0016-7061/

Previous studies have quantified modern soil loss from karst catchments using depression deposits. For example, Bai et al. (2010) estimated mean annual soil erosion rates from the Yongkang depression in the karst region of southwestern China during the past ~50 years by dating depression deposits using ^{137}Cs as a time-marker for 1963. However, as those studies were limited to the past ~50 years, they did not take into account the longer-term impacts of human activity upon sediment yield (Li et al., 2019a). The present status of rocky desertification in karst land might have been caused by modern human activity in the last 50 years but also by human activity much longer ago. Investigation of longer-term sediment yields may therefore improve our understanding of patterns of human activity causing rocky desertification in a historical context. No previous studies have examined the long-term variation in sedimentation rate in karst depressions and associated catchment sediment yield.

The anthropogenic radionuclide ^{137}Cs has been successfully used as a time-marker for 1963 in karst depressions (Bai et al., 2010). The radionuclides $^{210}Pb_{ex}$ (excess natural ^{210}Pb above mineralogical levels; Appleby et al., 1979; Mabit et al., 2014) and cosmogenic ^{14}C may be applied over timescales of ~100 years and > 100 years, respectively, but have not previously been used as chronometers for karst depressions, possibly because karst depression deposits have not been studied in detail, with soil loss and rocky desertification becoming areas of attention only in recent years (Jiang et al., 2014; Nian et al., 2018; Yan et al., 2019). Furthermore, cultivation disturbance means that it is more challenging to date deposits in karst depressions than in undisturbed sedimentation settings such as typical aquatic environments. This study attempted to date cultivated deposits using $^{210}Pb_{ex}$ and ^{14}C as tracers to reconstruct sedimentation chronologies over ≥100 years, thereby providing a new regime for dating karst depressions.

Overall, the objectives of this study were to (1) date deposits in a karst depression in the Three Gorges Reservoir Region (TGRR), China, using ^{137}Cs, $^{210}Pb_{ex}$, and ^{14}C to respectively obtain short-term (~50 years), medium-term (~100 years), and long-term (~600 years) sedimentation chronologies; (2) determine sedimentation rates (*SR*; cm yr^{-1}) in the depression and specific sediment yields (*SSY*; t ha^{-1} yr^{-1}; Vanmaercke et al., 2011) from the catchment during historical stages over the past 600 years; and (3) reconstruct the impact of long-term human activity on the changing sediment yields over the past 600 years. The results contribute to our understanding of long-term human impacts on soil loss at the depression-catchment scale and of the evolution and dynamics of rocky desertification in karst lands.

2. Materials and methods

2.1. The TGRR and study catchment

The TGRR (Fig. 1a) contains the main course and tributaries of the Yangtze River upstream of the Three Gorges Dam. The TGRR has a total area of 57,802 km^2 and supports a population density of ~350 people km^{-2} (Xiao et al., 2017). This region has a subtropical monsoon climate with high relative humidity, with a mean annual precipitation of ~1100 mm. Rainfall is variable, with 85% falling in the summer. Elevations range from 50 to 2948 m above sea level. The underlying bedrock comprises two major rock types, namely, purple/red sandstone (74%) and carbonate (19%) (Bao et al., 2015) (Fig. 1a). The carbonate rocks are extensively exposed and represent typical karst land of southern China, with some hill slopes having landscapes representing varying degrees of rocky desertification (Fig. 1a).

The TGRR is one of the most ecologically important and vulnerable regions in China. The region served as a passageway for several large-scale migrations from the end of the Yuan Dynasty to the Qing Dynasty in ancient China, including the well-known migration events from Huguang to Sichuan during the Ming and Qing dynasties. During these migration events, many people temporarily or permanently settled in the region, which led to deforestation for the purposes of fuel provision and land cultivation. This removal of vegetation resulted in large volumes of soil being eroded from hill slopes. In the late 1950s, large-scale tree felling occurred in many areas, with agricultural practices increasing soil erosion thereafter. These prolonged activities have contributed to rocky desertification.

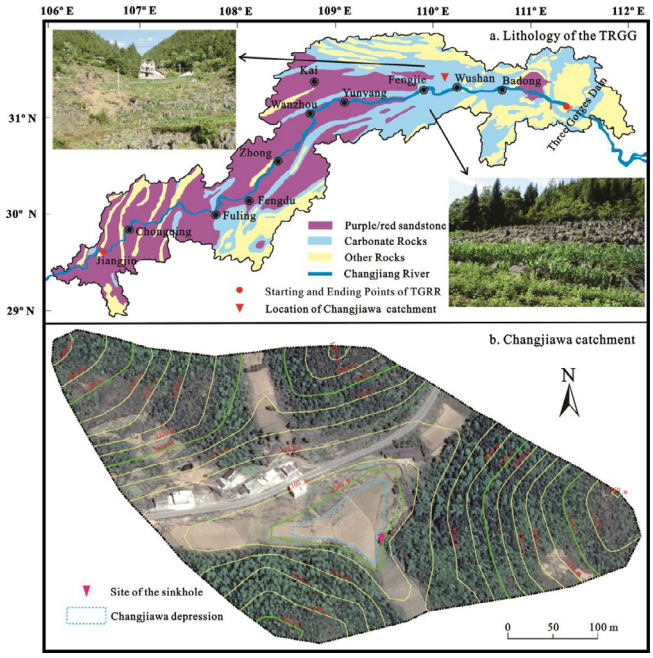

Fig. 1. (Top) Lithology of the TRGG and (Bottom) the Changjiawa catchment.

The Changjiawa catchment in Wushan County, including the depression and its broader catchment area, was selected as the study area (Fig. 1b). The depression has an area of ~0.38 ha, and the catchment area is 11.99 ha. The catchment has an elevation range of 1096–1163 m and comprises predominantly limestone, with a clasolite component of < 5%. A sinkhole is located near the southeastern border of the depression, at the foot of the hill slope. The calcareous soils are derived from these two rock types. The soil thickness is usually < 20 cm on the hill slopes but exceeds 300 cm in the depression. These calcareous soils are generally in direct contact with the underlying rock on the hill slopes and lack the intermediary weathering crusts common in non-karst regions. Trees such as pine (*Pinus massoniana*) and fir (*Cupressaceae*) covered the catchment before the 1950s. Most were felled for firewood in 1958 (corresponding to the time of the 'Great Leap Forward'), which was followed by restoration of grass and low brush. An aerial-seeding afforestation project was implemented during the 1980s, and there are presently some patches of croplands on the hill slopes adjacent to the depression. These patchy croplands are distributed among exposed limestone, whose presence demonstrates that the area has undergone a degree of rocky desertification (Fig. 2a). Most of the other hill slopes are covered by low forest and shrubs (Fig. 2b). The depression has been cultivated since the ancestors of the present residents arrived in the area ~600 years ago; crops are grown year-round, with maize (*Zea mays*) being grown in summer and autumn, and rapeseed (*Brassica napus*) in winter and spring. The depression commonly becomes waterlogged during heavy storms, with a water retention time of ~3 days. The floodwater recedes by flowing though the soil to reach bedrock fissures and entering underground river systems in the sinkhole.

2.2. Field sampling and laboratory analysis

Four sampling cores (1–4) were extracted from the Changjiawa depression using a manual corer (internal diameter 8 cm). Core 1 was taken near the depression center and cores 2–4 outward from there

a. Cropland on a hill slope. b. Low forest and shrubs.

Fig. 2. Representative landscape of the study catchment. Photographs by Y. Zhang.

(Fig. 3). Cores 1 and 2 were taken in December 2017, and cores 3 and 4 in April 2019. The top subsamples of the four cores, which were mixed by current tillage practices, were sectioned at ~9–15 cm intervals, and subsamples below this depth were sectioned at ~4–6 cm intervals. The lengths of cores 1–4 were 283, 291, 299, and 300 cm, respectively. All samples were freeze-dried, disaggregated, passed through a 2 mm mesh sieve, and weighed prior to analysis. ^{137}Cs and ^{210}Pb$_{ex}$ activities were determined in subsamples of the four cores from ≤120 cm depth. Organic matter (OM) content and sediment grain size were determined in all subsamples of Core 1. ^{137}Cs and ^{210}Pb$_{ex}$ activities were determined on a dry-weight basis using gamma spectrometry with a high-resolution, low-background, low-energy p-type coaxial germanium detector (GMX40P4, ORTEC), with counting times of > 80,000 s. Uncertainties were generally < 10% at the 95% confidence level. ^{137}Cs activity was determined using the 662 keV gamma ray; total ^{210}Pb activity using the 46.5 keV gamma ray; and ^{222}Rn (^{226}Ra decay product) activity using the 351.9 keV gamma ray of ^{214}Pb. ^{210}Pb$_{ex}$ activity was then calculated as the difference between the total ^{210}Pb and ^{214}Pb activities. OM content was determined using an element analyzer (Vario Macro Cube). The absolute grain size was determined using a laser particle size analyzer (Mastersizer 2000). The dry-sediment bulk density (γ, g cm^{-3}) of each subsample was calculated for Core 1 by dividing mass by volume.

^{14}C was measured only in Core 1, as this was located near the center of the depression and could well record the general sedimentation in the depression. Six bulk samples of charcoal fragments were extracted from six subsamples from depths of ≥100 cm, using a buoyancy technique (Fig. 4). Samples from this depth range were targeted because ^{14}C is generally applicable to ages greater than 100 years. No charcoal fragments were found at depths of 105–208 cm. To cover this gap, an additional core of 210 cm depth was recovered adjacent to Core 1. Two bulk samples of charcoal fragments from the new core were subjected to ^{14}C dating and the ages incorporated in the chronology of Core 1. The charcoal samples were freeze-dried to a constant weight and soaked in 1 M HCl for 24 h to remove carbonates. The samples were washed with ultrapure water 4–5 times to pH ~ 7, and freeze-dried again. Small pieces of charcoal were then carefully picked out with tweezers, and the remaining fine particles were discarded. Radiocarbon measurements were performed at the Accelerator Mass Spectrometry Center, Xi'an City, China, following the procedure described by Chen et al. (2018).

2.3. Dating methods

^{137}Cs, ^{210}Pb$_{ex}$, and ^{14}C dating methods were used conjointly to determine the short-, medium-, and long-term chronologies of the depression deposits, respectively. ^{137}Cs has been widely used to date undisturbed lake, reservoir, river floodplain, and estuary deposits by providing a reliable modern time-marker for 1963, corresponding to the year of maximum deposition of nuclear-weapon-derived radionuclides (Fig. 5a; Mabit et al., 2008, 2018; Navas et al., 2014). Karst depression deposits have commonly been subjected to long-term cultivation, and the marker ^{137}Cs peak of 1963 has therefore been disturbed and mixed in the tilled soils. Assuming that the annual tillage depth (d_0, cm) is constant over time, the tillage layer (0–d_0) would be elevated each year as new deposits were incorporated. The ^{137}Cs peak would have been mixed (by tilling) throughout the material within the tilling depth at 1963 and that deposited after 1963, resulting in little variation in ^{137}Cs activity within this depth range (0–D_0; D_0 = total depth tilled since 1963, cm; Fig. 5b). However, the ^{137}Cs activity of the material in this

a. Location of the sampling cores. b. Core extraction.

Fig. 3. Field sampling. Photographs by Y. Zhang.

Fig. 4. Charcoal fragment extraction. Photographs by Y. Zhang.

depth range would be higher than that in the underlying material (Fig. 5b). The bottom of the depth range in which ^{137}Cs activity is relatively high can be recognized as the time-marker of maximum ^{137}Cs fallout deposition in 1963 (Zhang et al., 2011) (Fig. 5b).

The $^{210}Pb_{ex}$ chronometer is generally used to date deposits in water bodies with continuous deposition over the past 100 years (Appleby et al., 1979). Detailed chronologies can be determined using models such as the Constant Initial Concentration model, the Constant Rate of Supply model, and the Composite Chronological model, which incorporates the ^{137}Cs time-marker (Appleby, 2008; Du and Walling, 2012; Zhang et al., 2015). Deposited $^{210}Pb_{ex}$ can also be disturbed and mixed by tillage through long-term cultivation, meaning that dating models appropriate for deposits in water bodies cannot be directly applied. However, the tillage layer (0–d_0) would be increased by fresh yearly sediment incorporation, with previously cultivated sediment at greater depths being buried under the present tillage layer and no longer subjected to continued disturbance. Radioactive equilibrium between total ^{210}Pb and supporting ^{226}Ra can be established in sediments buried over 100 years ago (~5 × half-life of ^{210}Pb), where the $^{210}Pb_{ex}$ activity should be virtually zero (Mabit et al., 2008, 2014). In the down-core profile, $^{210}Pb_{ex}$ activity decreases to near zero at the equilibrium depth indicating burial for ~100 years. Below that depth, the sediment has been buried for longer than 100 years, with the total ^{210}Pb activity already being in equilibrium with supporting ^{226}Ra. The equilibrium depth can thus be considered to be a time-marker for ~100 years before the sampling year.

^{14}C is generally used to date deposits such as aeolian accumulations, river terraces, alluvium, lacustrine sediments, and coastal deposits (e.g., Muscheler et al., 2014; Zhang et al., 2016; Nian et al., 2018; Putnam et al., 2019), although it may also be used as a chronometer for karst depressions. There are abundant sources of carbon fragments in the study region, including (1) crop straw and tree branches that were burnt as living fuels and then used as fertilizer for crop cultivation, (2) crop straw burnt on site and used as fertilizer, and (3) tree branches that were burnt during forest fires and transported with run-off and sediment into the depression. On the whole, plant ash used as fertilizer each year is the main source of the charcoal fragments. As for $^{210}Pb_{ex}$ deposition in the depression, these charcoal fragments can be mixed by tillage and buried under the constantly increasing tillage layer, with input of new sediment each year without further disturbance, thus

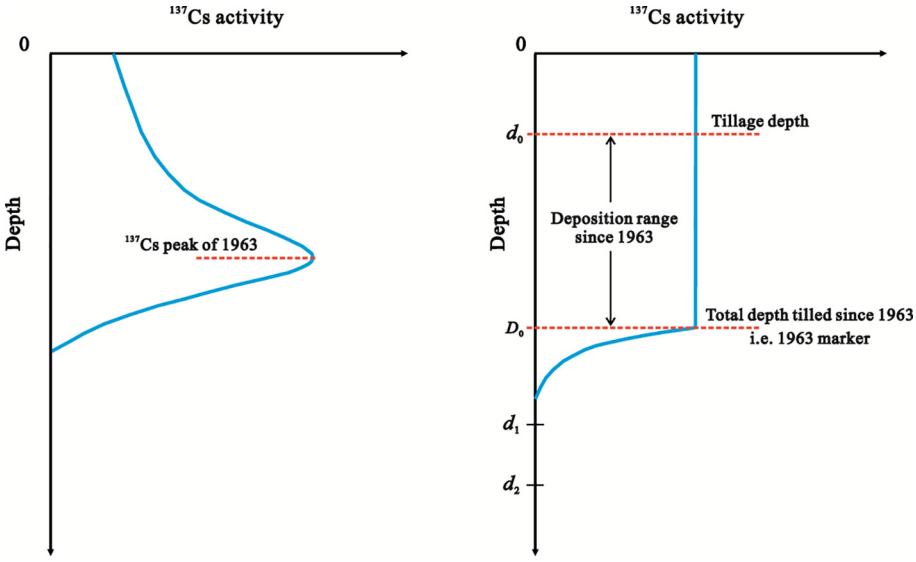

Fig. 5. Graphical illustration of the depth range of tilling since 1963.

providing a reliable chronology for depression deposits.

2.4. Calculating the historical SR and SSY

The average *SR* since the maximum ^{137}Cs deposition of 1963 can be calculated as:

$$SR_1 = \frac{D_0 - d_0}{Y - 1963} \quad (1)$$

where SR_1 is the average *SR* since 1963 (cm yr^{-1}), and Y is the sampling year.

Below depth D_0, the average *SR* during the time interval between years Y_2 and Y_1 can be calculated as:

$$SR_2 = \frac{d_2 - d_1}{Y_1 - Y_2} \quad (2)$$

where SR_2 is the average *SR* during the time interval Y_2 to Y_1 (cm yr^{-1}); d_1 and d_2 are depths in the core from the surface (cm) (Fig. 5b); and Y_1 and Y_2 are the dates (years) of the deposits at depths d_1 and d_2, respectively.

Once the *SR* in the depression have been calculated, the historical *SSY* values from the catchment can also be calculated. For the down-core depth of ~0–3 m, the variation in the area of the depression over time is negligible. The validity of this assumption was tested by drilling five small holes in the depression border area using a fine corer (internal diameter 2.7 cm), in addition to cores 1–4. The maximum depths (from the surface sediment to the bedrock) of the five holes were 276, 281, 293, 305, and 311 cm. Then, the historical SSY for each time interval can be calculated using:

$$SSY = \frac{100 \cdot SR \cdot \gamma \cdot a}{TE \cdot A} \quad (3)$$

where a is the depression area (ha); γ is the dry sediment bulk density (g cm^{-3}), determined from subsample weighted-mean values in Core 1; *TE* is the trap efficiency of the incoming sediment; and A is the catchment area (ha). As no monitoring data were available, the value of *TE* was assumed to be 0.7 based on a previous study of a depression with a similar sinkhole and floodwater retention time to that of the Changjiawa depression (Zhang et al., 2011).

3. Results

3.1. Measurement profiles

Measured ^{137}Cs, ^{226}Ra, total ^{210}Pb, and ^{210}Pb$_{ex}$ activities of the cores are shown in Fig. 6, and the OM content, γ, and particle-size distributions (clay, < 0.002 mm; silt, 0.002–0.020 mm; sand, 0.02–2.00 mm) in Core 1 are shown in Fig. 7. The ^{137}Cs activity is in the range 0–29 Bq kg^{-1} (Bq = becquerel, s^{-1}). The activity of cores 1–4 is higher in the uppermost 0–25, 0–32, 0–25, and 0–25 cm of the core sections, respectively, decreases with depth in the 25–33, 32–43, 25–32, and 25–40 cm section, respectively, and is negligible below these depths. The ^{226}Ra activity in the four cores varies between 24 and 33 Bq kg^{-1} and is nearly constant in the profiles. The total ^{210}Pb activity of the four cores ranges between 17 and 112 Bq kg^{-1}, and shows an overall decrease with depth. The activity of cores 1–4 at depths below 72, 75, 71, and 75 cm, respectively, is nearly constant and essentially equivalent to the value of ^{226}Ra. The ^{210}Pb$_{ex}$ activity of the four cores is in the range −8 to 86 Bq kg^{-1}, with values higher in upper than lower sections. The activity of cores 1–4 decreases to near zero with little variation below a depth of 72, 75, 71, and 75 cm, respectively. Negative values are related to ^{222}Rn emanation (Du and Walling, 2012). The depth patterns of ^{137}Cs and ^{210}Pb$_{ex}$ in the four cores indicate that the depth range of 0–120 cm was sufficient to cover the entire history of ^{137}Cs fallout since 1954, and ^{210}Pb$_{ex}$ deposition over the past 100 years or more. OM contents in Core 1 range between 11 and 26 g kg^{-1} with higher values above ~30 cm depth. There is a slight down-core increase in OM content between ~110 and ~184 cm depth, below which contents decrease. The particle composition and γ values show little variation throughout Core 1, which confirms the homogeneous nature of calcareous soil texture in karst regions (Zhang et al., 2018).

3.2. Core chronology, SR, and SSY

On the basis of the ^{137}Cs profiles, the 0–25, 0–32, 0–25, and 0–25 cm sections of cores 1–4, respectively, can be identified as the tilled-depth range since 1963 (0–D_0, Fig. 5b); consequently, the depths of 25, 32, 25, and 25 cm in cores 1–4, respectively, define the maximum ^{137}Cs fallout deposition, marking the year 1963 (Fig. 6). The depth of 72, 75, 71, and 75 cm in cores 1–4, respectively, where ^{210}Pb$_{ex}$ activity decreases down-core to almost zero (i.e. the total ^{210}Pb activity is essentially equal to the value of ^{226}Ra), can be considered the equilibrium depths marking a burial time of ~100 years ago (Fig. 6). To facilitate calculation and discussion, we disregard the differences in ^{210}Pb$_{ex}$ replenishment and decay associated with the different sampling times of December 2017 and April 2019, and define the time range of the past 100 years as 1917–2017 for all four cores. The depths of the 1963 ^{137}Cs marker in the four cores are largely consistent, with minor variations reflecting the spatial heterogeneity of sedimentation in the depression. This also applies to the 1917 ^{210}Pb$_{ex}$ markers in the four cores. Here we use the mean depth of the 1963 ^{137}Cs marker in the four cores to represent the depth of the 1963 layer in the depression (27 cm), and the mean 1917 ^{210}Pb$_{ex}$ marker depth to represent the depth of the 1917 layer in the depression (73 cm). Based on information from local residents, the constant tillage depth (d_0) is taken as ~15 cm.

The results of ^{14}C dating of Core 1 are shown in Fig. 8, along with the ^{137}Cs time-marker of 1963 (i.e., the mean 1963 ^{137}Cs marker depth in the four cores), and the ^{210}Pb$_{ex}$ time-marker of ~100 years ago, that is, 1917 (i.e., the mean 1917 ^{210}Pb$_{ex}$ marker depth in the four cores). Near the bottom of the core profile, three ^{14}C dates decrease in age upwards in the profile. Of these, the two dates of 1456 and 1463 are very close and can be considered the same date within analytical error (± 25 years). The dates 7665 BCE (227 cm depth), 1347 (208 cm depth), and 669 (100 cm depth) are anomalous because they violate the accepted pattern of chronological sedimentation whereby the oldest sediments should be at the bottom. The dates of 1351 (283 cm depth), 1463 (247 cm depth), 1702 (171 cm depth), and 1810 (142 cm depth) determined by ^{14}C dating, and 1917 (73 cm depth) and 1963 (27 cm) determined by ^{210}Pb$_{ex}$ and ^{137}Cs, respectively, are used to represent the chronology in the depression over the past 600 years and to estimate the historical *SR* and *SSY*. These chronologies are regarded as reliable because they follow the chronological sequence of sedimentation.

The *SR* and *SSY* value during the six stages can be calculated from chronologies using Eqs. (1)–(3). The calculated *SR* and *SSY* are relatively constant over the first three stages (1351–1462, 1463–1701 and 1702–1809), increase to their maximum values during the following two stages (1810–1916, 1917–1962), and finally decrease to their lowest values during the most recent stage (1963–2017; Table 1). The different *SR* and *SSY* values of the six stages largely reflect the changing intensity and pattern of sediment yields over the past 600 years.

4. Discussion

4.1. Higher sediment yields before 1963

SR and *SSY* values during the stages 1351–1462, 1463–1701, 1702–1809, 1810–1916, and 1917–1962 are higher than those of the most recent stage, 1963–2017, indicating a more intensive sediment yield before 1963. Two substantial migrations of people from Huguang to Sichuan have occurred in Chinese history, and human activity concurrent with these migrations can be considered to be responsible for

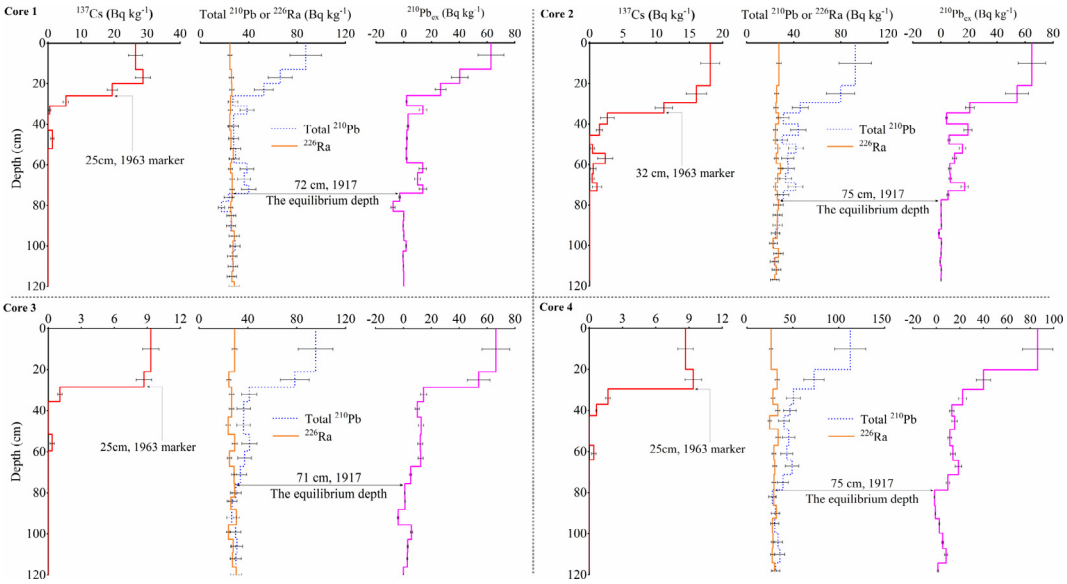

Fig. 6. Profiles of ^{137}Cs, ^{226}Ra, total ^{210}Pb, and $^{210}Pb_{ex}$ in the four studied cores.

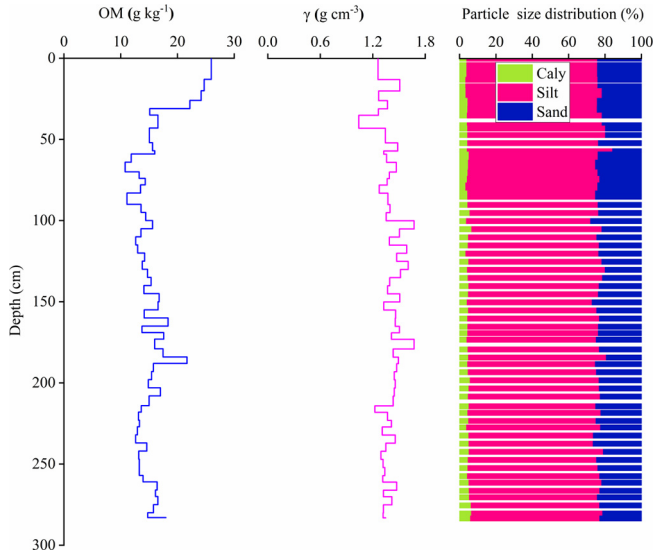

Fig. 7. Profiles of OM, γ, and particle size distribution in Core 1.

the high values before 1810. The first migration occurred between the end of the Yuan Dynasty and the beginning of the Ming Dynasty and involved the migration of war refugees and government-dominated migration between the Hongwu (1368) and Chenghua (1465) periods (Li, 1987; Cao, 1997; Yang, 1999). Historical records indicate that nearly 1.5 million people migrated from Hubei and nearby provinces to Sichuan province during this time (Yang, 1999). These records concur with information derived from local elders, who state that their ancestors were forced to migrate to the region from Hubei province during the Hongwu period (1368–1398) of the Ming Dynasty. Ancient salt mines are abundant in this region, and there was widespread deforestation as trees were felled for firewood to produce brine for salt production. Some hill slopes were cleared for cultivation as well. These activities would have increased the sediment yield from hilly regions, contributing to the high *SR* and *SSY* values in the period 1351–1462.

The second migration from Huguang to Sichuan occurred at the beginning of the Qing Dynasty, from the 33rd year of the Kangxi period (1694) to the 41st year of the Qianlong period (1776), and contributed to the high *SR* and *SSY* during 1463–1916. The extensive war from the end of the Ming Dynasty (1639) to the beginning of the Qing Dynasty (1680) reduced the population of Sichuan province from 4 million to just 0.6 million (Li, 1987). To promote the economic development of the Sichuan province, the Qing Dynasty government organized massive migration. More than 1 million people migrated from Hubei, Hunan, Shanxi, Yunnan, Guizhou, Guangxi, Jiangxi, Anhui, and other provinces. As occurred with the previous migration event, people cultivated the hill slopes and mined salt as they migrated, and many people settled permanently in the TGRR. Of note, maize was introduced to China from the Americas at the end of the 16th century, and made its way to the TGRR at the time of this migration (Chen et al., 2014). The resulting cultivation of maize would have contributed to soil loss on sloping land.

The relative constant *SR* and *SSY* over the first three stages (1351–1462, 1463–1701, and 1702–1809) might indicate that the disturbance intensity associated with migration was largely unchanged during this period. The higher values during 1810–1916 might reflect increasing disturbance such as deforestation and cultivation related to rapid population growth (Lu, 1991). The highest *SR* and *SSY* during 1917–1962 may record intensive deforestation in 1958 and a consistently increasing population. The previous disturbances may have affected some hill slopes at different times, but the deforestation of 1958 affected the entire catchment at once, with the impact of the former being relatively limited whereas deforestation triggered a massive catchment-wide increase in sediment yield.

4.2. Decreased sediment yield after 1963

The lower *SR* and *SSY* during the most recent stage of 1963–2017 indicate a substantially decreased sediment yield compared with earlier periods, particularly with respect to that during 1917–1962. This can be attributed to several factors: (1) human disturbance of the ecosystem decreased, and vegetation was somewhat restored during the 1960s and 1970s, with marked increases in grasses and shrubs during the early part of this period; (2) pine trees have grown following aerial-seeding afforestation during the 1980s; (3) the increased output of temporary rural workers lowered the intensity of ecosystem disturbance from the end of the 1990s; (4) the "Grain for Green" project has further restored local vegetation on steep (> 25°) slopes since 1998, with all current cultivation limited to more gentle (< 20°) slopes; and (5) most importantly, the previous intensive soil erosion triggered by human activity, and the low rate of new soil formation from the carbonate bedrock greatly reduced the amount of available erodible source materials

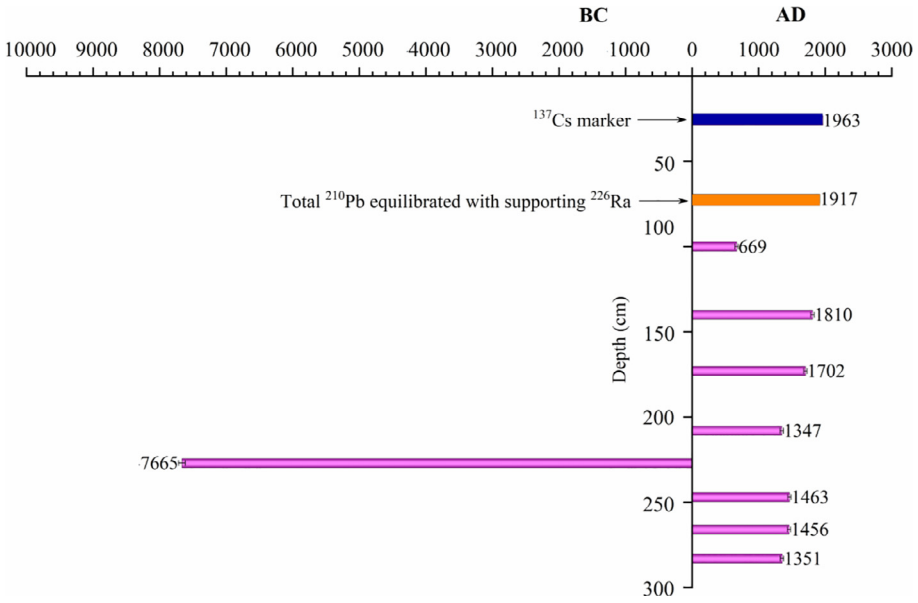

Fig. 8. Chronology derived from ^{14}C dating.

on hill slopes (Li et al., 2019a). Field surveys indicate that the soil layer on some hill slopes in the TGRR karst regions that are well covered by primitive local vegetation is thicker than ~100 cm, whereas that on hill slopes in the Changjiawa catchment is less than ~20 cm with high spatial heterogeneity. Previous human-triggered erosion exposed some bedrock. The outcropping rocks reduce the size of the erodible area, confine the remaining soils to the hill slopes and decrease the rate of soil loss. Local elders reported that few rock outcrops were seen on the hill slopes before the deforestation in 1958, whereas the intensive soil loss following the deforestation resulted in many rocks becoming exposed. Moreover, strategies to prevent soil loss, such as the construction of terraces, have been applied on slopes in some areas. The retention of soils in such areas further limited the sediment source. All of these characteristics greatly constrained the source material and restricted the sediment yield during 1963–2017. Bai et al. (2013) reported that the 1979 deforestation within the Shirenzhai depression catchment in southwestern China triggered a high SSY of 52.58 t ha^{-1} yr^{-1} during 1979–1990, which decreased to 2.56 t ha^{-1} yr^{-1} from 1991 to 2008 because the soils had been largely removed from the hill slopes and the remaining soils had been protected by terracing or vegetation rehabilitation.

The SSY of the Changjiawa catchment during 1963–2017 (~1.33 t ha^{-1} yr^{-1}) is higher than the soil loss tolerance range of 0.30–0.68 t ha^{-1} yr^{-1} in the karst area of southwestern China (Peng and Wang, 2012). Li et al. (2019b) reported SSY values for 40 karst catchments of various size of between 0.01 and 4.27 t ha^{-1} yr^{-1}, with a mean of ~0.91 t ha^{-1} yr^{-1}. Zhang et al. (2018) estimated the average SSY to be ~1.8 t ha^{-1} yr^{-1} since 1959 for a small karst catchment in the Yimeng Mountains region. The mean SSY of the Changjiawa catchment over the past 600 years is ~2.69 t ha^{-1} yr^{-1}, which is comparatively high. Field surveys indicate that thin layers of clasolites are interbedded with carbonate rocks in the hill slopes of the Changjiawa catchment. As the clasolite is more easily weathered but less soluble than the carbonate rocks, the clasolite contributes a greater amount per unit volume to the sediment source than do the carbonate rocks.

4.3. Factors controlling the changing pattern of sediment yield

SR and SSY values determined from the sediment core reflect the changing pattern of sediment yield from the Changjiawa catchment during the past 600 years. As discussed above, human activities have had a significant impact on sediment yield. In addition, rainfall can strongly influence erosion rates (Pruski and Nearing, 2002). Owing to the influence of the Little Ice Age and the weaker Asian monsoon, the intensity of precipitation in the TGRR during the Ming and Qing dynasties was lower than that of the modern period, with the annual precipitation displaying little variation over the past 100 years (Esper et al., 2002; Yang et al., 2013; Lü et al., 2014). However, the calculated *SR* in the Changjiawa depression and the catchment *SSY* since 1963 were lower than those of the five preceding stages, indicating that rainfall has not been the primary cause of changing sediment yield over the past 600 years.

Changes in sediment yield in various regions of China with well-documented erosion regimes are generally considered to be dominated by human activity. Such regions include the karst region of southwestern China, the black soil region of northeastern China, the rocky-mountain region of northern China, and the Loess Plateau (Wang et al., 2016; Fang and Sun 2017; Zhang et al., 2017, 2018, 2019; Li et al., 2019a). It is also likely that human activity over the past 600 years has controlled the changing pattern of sediment yield from the Changjiawa catchment.

4.4. Limitations and perspectives

Many potential uncertainties are associated with chronologies determined by ^{210}Pb$_{ex}$ and ^{14}C measurements. The uncertainty of ^{210}Pb$_{ex}$ dating is related to measurement errors of total ^{210}Pb and ^{214}Pb, which contribute to the error in ^{210}Pb$_{ex}$ activity in the sediment. In addition, the different ratios of sediment sources between surface soil and

Table 1
Historical *SR* and *SSY* values estimated from the cores.

Stage (AD)	1351–1462	1463–1701	1702–1809	1810–1916	1917–1962	1963–2017
SR (cm yr^{-1})	0.32 ± 0.10	0.31 ± 0.09	0.31 ± 0.09	0.64 ± 0.19	1.01 ± 0.30	0.22 ± 0.07
SSY (t ha^{-1} yr^{-1})	1.97 ± 0.79	1.95 ± 0.78	2.04 ± 0.81	4.04 ± 1.62	6.58 ± 2.63	1.33 ± 0.53

subsoils may result in depth variations of $^{210}Pb_{ex}$ activity in the core (Zhang et al., 2019). All this would influence the determination of the equilibrium depth (total ^{210}Pb equilibrated with supporting ^{226}Ra). Despite the uncertainties in the depth distributions of $^{210}Pb_{ex}$ activities in cores 1–4, some patterns are clear; e.g., the values decrease downcore, approach zero at depths of 72, 75, 71, and 75 cm, respectively, and show little variation at greater depths (Fig. 6).

Uncertainties in ^{14}C dating are attributed mainly to the diverse sources of carbon of different ages. As a result, the time of sediment deposition may differ from the age of the preserved carbon. In the case of ^{14}C dating of charcoal fragments, the anomalous chronologies of 7665 BCE (227 cm depth) in particular, as well as 1347 (208 cm depth) and 669 (100 cm depth), might suggest that older charcoal fragments were transported with the sediment derived from the hill slopes into the depression, where they mixed with new charcoal fragments conserved in the surface deposits. This process could have been driven by human activities such as deforestation or cultivation on the hill slopes. The hillslope soils may contain many historical charcoal fragments that are older than the timing of their erosion. It can be assumed that the disturbances related to mass migration and some later human activities triggered the transportation of older charcoal fragments with sediment from the hill slopes to the depression, resulting in the anomalous old ^{14}C dates. Furthermore, the relatively high OM contents in the depth range of ~150–200 cm, compared with adjacent parts of the depth profile, could have been induced by deforestation during the migration events. Deforestation can exacerbate the loss of surface soil, which is generally richer in OM than subsoil. Despite the uncertainty surrounding these more detailed interpretations, the findings of this first attempt to constrain sedimentation chronology in a karst depression using ^{14}C dating indicate the merits of this approach.

The six successive stages considered in this study are of different durations. The longer the duration of the stage, the less detailed the interpretation of human impact on the *SR* (or *SSY*) that can be inferred from the sediment core data. In particular, *SR* (or *SSY*s) at some times during the stage 1463–1701 might have been higher or lower than the mean value of the entire time interval. For example, the *SR* (or *SSY*) might have been lower during the extensive war that marked the transition from the Ming Dynasty to the Qing Dynasty (1639–1680) because of the sharp decline in population, but this detailed human impact on soil loss cannot be conclusively inferred from the mean *SR* (or *SSY*) estimated over the entire time interval.

The inferred tillage depth of 15 cm is based on the traditional tillage regime, which could be expected to represent the general tillage depth in the depression. Significant variations in the tillage depth could influence dating results. Nevertheless, the chronologies of the four cores determined by ^{137}Cs and $^{210}Pb_{ex}$ are largely consistent, indicating that any variations in tillage depth had little influence on the chronology. In addition, ^{14}C dates determined from Core 1 do not reflect the spatial variability in sedimentation across the depression. Theoretically, more core ^{14}C dates could be expected to yield more representative results, although costs would increase accordingly. Indeed, considering the small size of the depression, the analysis of single-core ^{14}C dates from the center of the depression, together with the four cores of ^{137}Cs and $^{210}Pb_{ex}$ time markers, could reflect historical patterns of sedimentation in the depression and sediment yield from the catchment.

Nevertheless, our results suggest that human activity during the period 1351–1962 triggered more intensive soil loss than that during the period since 1963. The rocky desertification of karst environments might thus be a long-term land-surface process influenced by human activity on timescales of several hundred years rather than being a short-term process of several decades. Investigations of more depression deposits with higher time resolution would help to confirm the findings of the present study and provide more details regarding the long-term impacts of historical human activity on sediment yield from karst catchments.

5. Conclusion

This is the first attempt to use dated depression deposits to examine the long-term human impact (600 years) on sediment yields from a small karst catchment. Based on the chronologies determined by the combined use of ^{137}Cs, $^{210}Pb_{ex}$, and ^{14}C chronometers, we calculated historical *SR* and *SSY* values of the catchment using samples from four sediment cores. The obtained values suggest that the soil loss from 1351 to 1962 was more intensive than that of the modern age since 1963. The changing pattern of *SR* and *SSY* values reflects the impacts of human activity on sediment yield from the karst catchment over the past 600 years, and further suggests that rocky desertification is a long-term land-surface process caused by human activity over periods of > 100 years, rather than a short-term modern process occurring over several decades.

Declaration of Competing Interest

The authors declare that they have no known competing financial interests or personal relationships that could have appeared to influence the work reported in this paper.

Acknowledgments

This work was supported financially by the National Key Research Program of China (2016YFC0502301) and the National Natural Sciences Foundation of China (Grant numbers 41671277 and 41873025).

References

Appleby, P.G., 2008. Three decades of dating recent sediments by fallout radionuclides: a review. Holocene 18, 83–93. https://doi.org/10.1177/0959683607085598.

Appleby, P.G., Oldfield, F., Thompson, R., Huttunen, P., 1979. ^{210}Pb dating of annually laminated lake sediments from Finland. Nature 280, 53–55. https://doi.org/10.1038/280053a0.

Bai, X., Zhang, X., Chen, H., He, Y., 2010. Using ^{137}Cs fingerprint technique to estimate sediment deposition and erosion rates from Yongkang depression in karst region of Southwest China. Land Degrad. Dev. 21, 474–479. https://doi.org/10.1002/ldr.983.

Bai, X., Zhang, X., Long, Y., Liu, X., Zhang, S., 2013. Use of ^{137}Cs and $^{210}Pb_{ex}$ measurements on deposits in a karst depression to study the erosional response of a small karst catchment in Southwest China to land-use change. Hydrol. Process. 27, 822–829. https://doi.org/10.1002/hyp.9530.

Bao, Y., Gao, P., He, X., 2015. The water-level fluctuation zone of Three Gorges Reservoir—a unique geomorphological unit. Earth-Sci. Rev. 150, 14–24. https://doi.org/10.1016/j.earscirev.2015.07.005.

Cao, S., 1997. History of China. The fifth volume. Fujian people press pp 153 and pp 158. (In Chinese).

Chen, J., Yang, H., Zeng, Y., Guo, J., Song, Y., Ding, W., 2018. Combined use of radiocarbon and stable carbon isotope to constrain the sources and cycling of particulate organic carbon in a large freshwater lake. China. Sci. Total Environ. 625, 27–38. https://doi.org/10.1016/j.scitotenv.2017.12.275.

Chen, Y., Huang, Y., Zhou, Y., 2014. Does the Columbian exchange end the climate induced peace-turbulence cycle?—a historical investigation on the correlation between China's maize planting and peasant revolts. China Econ. Quart. 13, 1215–1238. https://doi.org/10.13821/j.cnki.ceq.2014.03.002. (In Chinese with English abstract).

Du, P., Walling, D.E., 2012. Using ^{210}Pb measurements to estimate sedimentation rates on river floodplains. J. Environ. Radioact. 103 (1), 59–75. https://doi.org/10.1016/j.jenvrad.2011.08.006.

Dai, Q., Peng, X., Yang, Z., Zhao, L., 2017. Runoff and erosion processes on bare slopes in the Karst Rocky Desertification Area. Catena 152, 218–226. https://doi.org/10.1016/j.catena.2017.01.013.

Esper, J., Cook, E.R., Schweingruber, F.H., 2002. Low-frequency signals in long tree-ring chronologies for reconstructing past temperature variability. Science 295, 2250–2253. https://doi.org/10.1126/science.1066208.

Fang, H., Sun, L., 2017. Modelling soil erosion and its response to the soil conservation measures in the black soil catchment, Northeastern China. Soil Tillage Res. 165, 23–33. https://doi.org/10.1016/j.still.2016.07.015.

Ford, D., Williams, P.D., 2013. Karst Hydrogeology and Geomorphology. John Wiley & Sons, Chichester.

Jiang, Z., Lian, Y., Qin, X., 2014. Rocky desertification in Southwest China: impacts, causes, and restoration. Earth-Sci. Rev. 132, 1–12. https://doi.org/10.1016/j.earscirev.2014.01.005.

Li, S., 1987. History of Sichuan population. Sichuan people press, Chengdu (In Chinese).

Li, Z., Xu, X., Liu, M., Li, X., Zhang, R., Wang, K., Xu, C., 2017. State-space prediction of

spring discharge in a karst catchment in southwest China. J. Hydrol. 549, 264–276. https://doi.org/10.1016/j.jhydrol.2017.04.001.
Li, Z., Xu, X., Xu, C., Liu, M., Wang, K., 2018. Dam construction impacts on multiscale characterization of sediment discharge in two typical karst watersheds of southwest China. J. Hydrol. 558, 42–54. https://doi.org/10.1016/j.jhydrol.2018.01.034.
Li, Z., Xu, X., Zhang, Y., Wang, K., Zeng, P., 2019a. Reconstructing recent changes in sediment yields from a typical karst watershed in southwest China. Agr. Ecosyst. Environ. 269, 62–70. https://doi.org/10.1016/j.agee.2018.09.024.
Li, Z., Xu, X., Zhu, J., Xu, C., Wang, K., 2019b. Sediment yield is closely related to lithology and landscape properties in heterogeneous karst watersheds. J. Hydrol. 568, 437–446. https://doi.org/10.1016/j.jhydrol.2018.10.076.
Lu, L., 1991. Wushan Conty Chronicle. Sichuan people press, Chengdu (In Chinese).
Lü, J., Zhu, C., Ju, J., Lin, X., 2014. Interdecadal variability in summer precipitation over East China during the past 100 years and its possible causes. Chin. J. Atmos. Sci. 38 (4), 782–794. https://doi.org/10.3878/j.issn.1006-9895.1401.13227. (In Chinese with English abstract).
Mabit, L., Benmansour, M., Walling, D.E., 2008. Comparative advantages and limitations of Fallout radionuclides (^{137}Cs, ^{210}Pb and ^{7}Be) to assess soil erosion and sedimentation. J. Environ. Radioact. 99, 1799–1807. https://doi.org/10.1016/j.jenvrad.2008.08.009.
Mabit, L., Benmansour, M., Abril, J.M., Walling, D.E., Meusburger, K., Iurian, A.R., Bernard, C., Tarjánh, S., Owens, P.N., Blake, W.H., Alewell, C., 2014. Fallout ^{210}Pb as a soil and sediment tracer in catchment sediment budget investigations: a review. Earth-Sci. Rev. 138, 335–351. https://doi.org/10.1016/j.earscirev.2014.06.007.
Mabit, L., Bernard, C., Yi, A.L.Z., Fulajtar, E., Dercon, Gerd, Zaman, M., Toloza, A., Heng, L., 2018. Promoting the use of isotopic techniques to combat soil erosion: an overview of the key role played by the SWMCN Subprogramme of the Joint FAO/IAEA Division over the last 20 years. Land Degrad. Dev. 29, 3077–3091. https://doi.org/10.1002/ldr.3016.
Navas, A., López-Vicente, M., Gaspar, L., Palazón, L., Quijano, L., 2014. Establishing a tracer-based sediment budget to preserve wetlands in Mediterranean mountain agroecosystems (NE Spain). Sci. Total Environ. 496, 132–143. https://doi.org/10.1016/j.scitotenv.2014.07.026.
Muscheler, R., Adolphi, F., Svensson, A., 2014. Challenges in ^{14}C dating towards the limit of the method inferred from anchoring a floating tree ring radiocarbon chronology to ice core records around the Laschamp geomagnetic field minimum. Earth Planet. Sc. Lett. 394, 209–215. https://doi.org/10.1016/j.epsl.2014.03.024.
Nian, X., Zhang, W., Wang, Z., Sun, Q., Chen, J., Chen, Z., Hutchinson, S.M., 2018. The chronology of a sediment core from incised valley of the Yangtze River delta: comparative OSL and AMS ^{14}C dating. Mar. Geol. 395, 320–330. https://doi.org/10.1016/j.margeo.2017.11.008.
Putnam, A.E., Bromley, G.R.M., Rademaker, K., Schaefer, J.M., 2019. In situ ^{10}Be production-rate calibration from a ^{14}C-dated late-glacial moraine belt in Rannoch Moor, central Scottish Highlands. Quat. Geochronol. 50, 109–125. https://doi.org/10.1016/j.quageo.2018.11.006.
Peng, T., Wang, S., 2012. Effects of land use, land cover and rainfall regimes on the surface runoff and soil loss on karst slopes in southwest China. Catena 90, 53–62. https://doi.org/10.1016/j.catena.2011.11.001.
Pruski, F., Nearing, M., 2002. Climate-induced changes in erosion during the 21st century for eight US locations. Water Resour. Res. 38https://doi.org/10.1029/2001WR000493. 34–1–34-11.
Vanmaercke, M., Poesen, J., Verstraeten, G., Vente, D., Ocakoglu, F., 2011. Sediment yield in Europe: spatial patterns and scale dependency. Geomorphology 130, 142–161. https://doi.org/10.1016/j.geomorph.2011.03.010.
Wang, S., Fu, B., Ciais, P., Piao, S., Wang, S., Feng, X., Wang, Y., Lü, Y., 2016. Reduced sediment transport in the Yellow River due to anthropogenic changes. Nat. Geosci. 9, 38–41 https://doi.org/doi.org/10.1038/ngeo2602.
Wang, S., Liu, Q., Zhang, D., 2004. Karst rock desertification in Southwestern China: geomorphology, land use, impact and rehabilitation. Land Degrad. Dev. 15, 115–121. https://doi.org/10.1002/ldr.592.
Xiao, Q., Hu, D., Xiao, Y., 2017. Assessing changes in soil conservation ecosystem services and causal factors in the Three Gorges Reservoir region of China. J. Clean. Prod. 163, s172–s180. https://doi.org/10.1016/j.jclepro.2016.09.012.
Yan, Y., Dai, Q., Wang, X., Jin, L., Mei, L., 2019. Response of shallow karst fissure soil quality to secondary succession in a degraded karst area of southwestern China. Geoderma 348, 76–85. https://doi.org/10.1016/j.geoderma.2019.04.017.
Yang, G., 1999. Migration and cultivation in the hilly region of Exi in the Ming and Qing dynasties. Hist. Chin. Agric. 18, 17–28 (In Chinese).
Yang, J., Nie, Y., Chen, H., Wang, S., Wang, K., 2016. Hydraulic properties of karst fractures filled with soils and regolith materials: implication for their ecohydrological functions. Geoderma 276, 93–101. https://doi.org/10.1016/j.geoderma.2016.04.024.
Yang, X., Chen, F., Yuan, D., Cheng, H., Zhang, Y., Huang, F., 2013. Climate change during Little Ice Age with high-resolution stalagmite record in the Three-Gorges Reservoir Area. Sci. Geog. Sinic. 33, 629–634. https://doi.org/10.13249/j.cnki.sgs.2013.05.629. (In Chinese with English abstract).
Yuan, D., 2006. The development of Modern Karstology in China. Geol. Rev. 52, 733–736 (In Chinese with English abstract).
Zhang, J., Ma, X., Qiang, M., Huang, X., Li, S., Guo, X., Henderson, A.C.G., Holmes, A., Chen, F., 2016. Developing inorganic carbon-based radiocarbon chronologies for Holocene lake sediments in arid NW China. Quaternary Sci. Rev. 144, 66–82. https://doi.org/10.1016/j.quascirev.2016.05.034.
Zhang, X., Bai, X., Liu, X., 2011. Application of a ^{137}Cs fingerprinting technique for interpreting responses of sediment deposition of a karst depression to deforestation in the Guizhou Plateau, China. Sci. China Earth Sci. 54, 431–437. https://doi.org/10.1007/s11430-010-4105-x.
Zhang, X., Zhang, G., Garbrecht, J.D., Steiner, J.L., 2015. Dating sediment in a fast sedimentation reservoir using cesium-137 and lead-210. Soil Sci. Soc. Am. J. 79, 948–956. https://doi.org/10.2136/sssaj2015.01.0021.
Zhang, Y., Liao, J., Long, Y., An, J., Xu, S., Wang, X., 2018. Dating reservoir deposits to reconstruct sediment yields from a small limestone catchment in the Yimeng Mountain region, China. Catena 166, 1–9. https://doi.org/10.1016/j.catena.2018.03.012.
Zhang, Y., Long, Y., Li, B., Xu, S., Wang, X., Liao, J., 2017. Use of reservoir deposits to reconstruct the recent changes in sediment yields from a small granite catchment in the Yimeng Mountain region, China. Geomorphology 293, 167–177. https://doi.org/10.1016/j.geomorph.2017.05.017.
Zhang, Y., Long, Y., Lu, X., Wu, Z., Xu, S., Wang, X., Li, W., 2019. Dating reservoir deposits to assess the recently changing sediment yields from a medium-sized agricultural catchment. Land Degrad. Dev. 2019, 1–15. https://doi.org/10.1002/ldr.3391.